

Journal Pre-proof

Luminescence dating of holocene siliciclastic sediments in eastern Dahomey Basin, southwestern Nigeria

Richard O. Fakolade, Philip R. Ikhane, Qiuyue Zhao, Qingzhen Hao, Helena Alexanderson, Zhengtang Guo



PII: S1040-6182(21)00323-2

DOI: <https://doi.org/10.1016/j.quaint.2021.05.024>

Reference: JQI 8904

To appear in: *Quaternary International*

Received Date: 28 December 2020

Revised Date: 27 May 2021

Accepted Date: 27 May 2021

Please cite this article as: Fakolade, R.O., Ikhane, P.R., Zhao, Q., Hao, Q., Alexanderson, H., Guo, Z., Luminescence dating of holocene siliciclastic sediments in eastern Dahomey Basin, southwestern Nigeria, *Quaternary International* (2021), doi: <https://doi.org/10.1016/j.quaint.2021.05.024>.

This is a PDF file of an article that has undergone enhancements after acceptance, such as the addition of a cover page and metadata, and formatting for readability, but it is not yet the definitive version of record. This version will undergo additional copyediting, typesetting and review before it is published in its final form, but we are providing this version to give early visibility of the article. Please note that, during the production process, errors may be discovered which could affect the content, and all legal disclaimers that apply to the journal pertain.

© 2021 Published by Elsevier Ltd.

1 **Luminescence Dating of Holocene Siliciclastic Sediments in Eastern Dahomey Basin,**
2 **Southwestern Nigeria**

3 Richard O. Fakolade¹, Philip R. Ikhane², Qiuyue Zhao³, Qingzhen Hao^{4,5,6,7,*}, Helena
4 Alexanderson^{8,9}, Zhengtang Guo^{4,5,6,7}

5 ¹ Department of Mineral and Petroleum Resources Engineering technology, School of
6 engineering, The Federal Polytechnic Ado Ekiti, Nigeria

7 ² Department of Earth Sciences, Faculty of Science, Olabisi Onabanjo University Ago Iwoye
8 Nigeria

9 ³ Key Laboratory of Tourism and Resources Environment in Universities of Shandong,
10 Taishan University, Taian, China

11 ⁴ Key Laboratory of Cenozoic Geology and Environment, Institute of Geology and
12 Geophysics, Chinese Academy of Sciences, China

13 ⁵ Center for Excellence in Life and Palaeoenvironment, Chinese Academy of Sciences, China

14 ⁶ Innovation Academy for Earth Science, Chinese Academy of Sciences, China

15 ⁷ University of Chinese Academy of Science, China

16 ⁸ Department of Geology, Lund University, Sweden

17 ⁹ Department of Geosciences, UiT the Arctic University of Norway, Norway

18 * Corresponding author

19 E-mail address: haoqz@mail.iggcas.ac.cn

20 **Abstract**

21 Several attempts at reconstructing geological settings and palaeoclimatic changes of the
22 siliciclastic deposits of the Dahomey Basin, SW Nigeria, using relative age dating and
23 correlation methods, have resulted in serious discrepancies on the ages. Therefore, a
24 chronology framework established by an absolute age dating method is requisite to constrain
25 the geological interpretation. This research focuses on quartz optically stimulated
26 luminescence (OSL) dating of the upper siliciclastic sediments to help bridge the lacuna that
27 arose from previous relative geologic dating. Ten sub-surface sediment samples were
28 collected from the eastern part of the basin, and quartz OSL dating using single-aliquot
29 regenerative-dose protocol was conducted for all the samples. The OSL signals appear well
30 bleached prior to deposition and the OSL ages are reliable and robust. Through the
31 application of OSL, the age framework of the uppermost part of sediments in the study area

32 was established. The OSL dating results revealed that these depositional periods fall within
33 the Holocene and are concentrated during two groups: 3.52 ka–1.55 ka, and 0.64 ka–0.05 ka.
34 The samples with ages of 3.52 ka–1.55 ka distribute in the belt-like inland zone
35 approximately parallel to the coastline. This deposition episode appears to be caused by the
36 decrease in relative sea level during late Holocene. Thus, this study sheds light on the
37 understanding past coast dynamics in the region.

38 **Keywords:** Luminescence dating; Quaternary; Holocene; Dahomey Basin; Nigeria

39 **1. Introduction**

40 Various research work has been conducted within the Dahomey Basin due to their geologic
41 peculiarity and economic importance (Adegoke, 1980). Exploration of bitumen, limestone,
42 glass sands and phosphates (Nton et al., 2006) has been undertaken with discovery of crude
43 oil in 1908 (Billman, 1982). This has sprung up great geological interest for further research
44 in the basin for hydrocarbon potential (Elueze and Nton, 2004). The knowledge of age of the
45 deposits will provide crucial information for future exploration of these natural resources and
46 understanding the evolution of coastal environment in the Dahomey Basin.

47 Previous researches had postulated ages for the sediments in the Dahomey Basin through the
48 application of series of relative age dating approaches, including age correlation of the basin
49 (Jones and Hockey, 1964; Reymont, 1965), dating of available pollen (Agagu, 1985) and
50 paleontological approach (Adegoke, 1969; Olabode and Mohammed, 2016). This has resulted
51 in serious age discrepancies ranging from Maastrichtian to Quaternary ages (Olabode et al.,
52 2016). Hence, there is an urgent need to adopt absolute age dating method to resolve and
53 bridge the lacuna arising from the various age differences of the siliciclastic deposits.

54 Optically simulated luminescence (OSL) is one of the most intensively and veritably used
55 numerical dating techniques to determine the age of Late Quaternary sub-surface sediments
56 (Murray and Wintle, 2000, 2003; Wintle and Murray, 2006; Chen et al., 2015; Zhang et al.,
57 2018). OSL dating techniques (Duller, 2004; Olley et al., 1998, 1999) work well not only on
58 sediments where grains have adequate exposure to sunlight at the time of deposition (Rhodes,
59 2007), but also on samples which were poorly bleached prior to sedimentation (Zhao et al.,
60 2015, 2017). It is applied by estimating the impact of radiation on the crystalline structure of
61 quartz mineral mostly presented in all sedimentary environments isolated from light (Wintle,
62 1997, 2008; Murray and Wintle, 2000, 2003). The OSL signal observed from quartz revealed

63 several exponentials relative to different levels of traps (Bailey et al., 1997) and successful
64 OSL dating is dependent on a fast signal component (Murray and Wintle 2000). This research
65 aims to determine the age of the uppermost alluvial deposits in the eastern Dahomey Basin to
66 help bridge the long touted age disparities of the formation in previous research (Jones and
67 Hockey, 1964; Agagu, 1985; Omatsola and Adegoke, 1981).

68 **2. Geologic and tectonic settings of the Dahomey Basin**

69 The Dahomey Basin, also called Benin Embayment, is located on the shore of West Africa
70 (Whiteman, 1982), with coordinate of latitude 6°10'N to 6°25' N and longitude 4°30' E to
71 4°50' E respectively (Fig. 1). It is a rift or marginal pull-apart basin (Whiteman, 1982) or
72 marginal sag basin (Kingston et al., 1983), part of the West African pre-cratonic basins
73 (Mpanda, 1997) which was initiated during the early Cretaceous separation of the South
74 American and African plates, and opening of the South Atlantic Ocean (Adegoke, 1980;
75 Omatsola and Adegoke, 1981). The Dahomey Basin is a combination of inland, coastal,
76 offshore settings that stretches from southeastern Ghana through Togo and the Republic of
77 Benin to southwestern trending along the east-west direction in Nigeria, with Cretaceous
78 strata along the shore estimated to be about 200 m thick (Okosun, 1990; Olabode and
79 Mohammed, 2016). The geologic, stratigraphic, sedimentological and organic geochemical
80 studies of different parts of the alluvial deposits in the Dahomey Basin have been reported
81 (e.g., Idowu et al, 1993; Adekeye, 2004; Adekeye et al., 2006; Nton et al., 2006; Ikhane et al.,
82 2014).

83 The study area is located in eastern part of the Dahomey Basin, in the area or vicinity of Ilaje
84 community in coastal environment of Ondo state (Fig. 1). The coastal vegetation along the
85 beach is dominate mangrove (Awosika and Folorunsho, 2010) with some coconut trees,
86 palms, sedges and climbers. The study area is a barrier lagoon coastal complex (Woodroffe
87 and Horton, 2005; Awosika and Folorunsho, 2010), stretching from around Agerige
88 community where the coastline starts a southward variation. It consists of beach ridges
89 adjoined with a foreshore of more than 50 m above the sea level similar to that of modern
90 coast. The beach crest elevation generally ranges from 3 to 4 m above mean water level.
91 Relief ranges from sea level along the coast backed by a wide expanse of tidal flat with the
92 coastal plain relief rising gently from 2 m to about 50 m above mean sea level. This barrier
93 lagoon bar experiences tides, current waves and predominantly of long shore currents
94 generated by south-westerly breaking waves at various degrees. Though the tidal range is

95 relatively small, the effects of tides on the general morphology of the coastline are very
96 significant.

97 The alluvial sediments here were previously inferred a Pleistocene or Holocene age by
98 relative dating (Omatsola and Adegoke, 1981; Agagu, 1985). The alluvial plain is
99 lithologically indistinguishable from typical coastal plain sands strata. The high-level terraces
100 are rarely exposed, although few sections were seen around Ofada and Moloki on the Ogun
101 River bank. The sediments are made up of medium to slightly fine grained, well sorted to
102 moderately well sorted sands. Quaternary sediments mainly consist of recent alluvium
103 (Agagu, 1985), underlain by siltstone/ mudstone described by Omatsola and Adegoke (1981).

104 **3. Materials and methods**

105 **3.1 Materials**

106 In this study, 10 representative samples were collected from the study area in the eastern
107 Dahomey Basin (Fig. 1). The samples are from sub-surface and unconsolidated in nature.
108 Texturally, the samples are fine to coarse grained sand with an average 85.0% of the samples
109 being medium grained sand. The colour ranges from white to light greyish and brownish red,
110 an indication of high impurities. During sampling, surface sediments were removed, then the
111 stainless-steel tube with 30 cm long and 5 cm diameter was hammered to allow the sample
112 fill the tube. The tube was sealed at both ends using aluminum foil and wrapped with the
113 black nylon to prevent it from sunlight reflection. Then each of the samples was properly
114 preserved in a sealed opaque container and clearly labelled for laboratory analysis.

115 **3.2 OSL dating method**

116 The single-aliquot regenerative dose (SAR) protocol was widely adopted to determine the
117 equivalent dose (D_e) of quartz samples (Murray and Wintle, 2000; Roberts and Duller, 2004;
118 Lai and Wintle, 2006; Rodnight, et al., 2006; Wang et al., 2006; Roberts, 2007; Lai, 2010;
119 Chen et al., 2012). This can then be calculated from the ratio of the natural and regenerated
120 luminescence signals (Murray and Wintle, 2003; Yang et al., 2014). Both natural and
121 regenerative signals (Buylaert et al., 2008; Kang et al., 2013) are normalized with a
122 successive test dose which are used to monitor and correct for a potential sensitivity change.
123 This radiation (α , β and γ) from the radionuclides in the mineral and its natural environment
124 determined by either gamma spectrometry, neutron activation analysis, or alpha counting
125 (Aitken, 1985; Guérin et al., 2012) can be converted into alpha, beta and gamma dose rate
126 using conversion factors (Stokes et al., 2001; Chen et al., 2012).

127 3.2.1 Sample pretreatment

128 Preparation of the samples and OSL experiments were conducted under a subdued red light in
129 the luminescence dating laboratory, Key Laboratory of Tourism and Resources Environment
130 in Universities of Shandong, Taishan University, Taian City, China. The two outer ends of
131 each sample in the steel tube were removed for water content and dose rate analysis, while
132 the remaining sediment was pretreated for luminescence measurement.

133 The remaining samples in the middle part of the tube were pretreated following the routine
134 procedures, including treatment with 10% HCl and 10% H₂O₂ to remove carbonate and
135 organic matter, respectively. After wet sieving, grains in the range of 150–250 μm were
136 extracted. The coarse fraction was then cleaned with 10% HF for 20 minutes to remove
137 coatings and the outer alpha irradiated layer, and rinsed in 10% HCl to remove any
138 precipitated fluorides. Subsequently, the remaining grains were separated by heavy liquid to
139 extract quartz grains ($2.62 < \rho < 2.75 \text{ g/cm}^3$). The purity of quartz was checked by IR
140 depletion ratio method (Duller, 2003) and 110 °C TL peak (Jain et al., 2004). The quartz
141 grains of each sample were mounted as small (2mm diameter) aliquots on a stainless-steel
142 discs, and twelve discs were measured for each sample.

143 3.2.2 Dose rate determination

144 Determination of the sediment dose rate involves assessment of concentrations of U, Th and
145 K in the sample, water content and cosmic ray dose contribution. The environmental dose
146 rate was determined by the U, Th and K concentrations, measured by neutron activation
147 analysis (NAA) method in the Chinese Atomic Energy Institute. The U, Th and K
148 concentrations were converted to dose rates (Aitken, 1998). The total environmental dose
149 rate, including the contribution from cosmic radiation, was calculated according to Adamiec
150 and Aitken (1998). The cosmic ray dose contribution was estimated as a function of
151 longitude, latitude, altitude and depth (Prescott and Hutton, 1994). The in situ water content
152 was measured by weighing the sample before and after drying (mass of moisture/dry mass),
153 and was assigned an absolute uncertainty of ±5%.

154 3.2.3 Equivalent doses determination

155 D_e were estimated using the improved SAR protocol (Murray and Wintle, 2000, 2003; Wintle
156 and Murray, 2006; Rittenour 2008). Its determination includes irradiation, preheating and
157 stimulating procedures. The procedures were conducted using an automated Risø TL/OSL
158 DA-20 reader equipped with blue LEDs (470 nm, ~80 mW cm⁻²) and infrared LEDs (875 nm,

159 $\sim 135 \text{ mW cm}^{-2}$) (Bøtter-Jensen et al., 1994; Stokes, 1999). The irradiation procedure adopted
160 a $^{90}\text{Sr}/^{90}\text{Y}$ beta source which was fitted on the reader with a dose rate of $\sim 0.10 \text{ Gy/s}$ to quartz
161 grains in stainless steel discs. The preheating was set at $160 \text{ }^\circ\text{C}$ for 20 s, based on the preheat
162 plateau and thermal transfer tests. The optical stimulation was conducted using blue light-
163 emitting diodes (LEDs) for 40 s at $125 \text{ }^\circ\text{C}$. This was detected using a 9235QA
164 photomultiplier tube through a 7.5 mm thick U-340 filter. The OSL signals for the D_e
165 determination were derived from the first 0.64 s stimulation minus a background of the
166 following 0.64 s of stimulation.

167 Preheat plateau test was carried out on samples MHN R2 and ARR R4 to show the variation
168 in dose with different preheats. The aliquots were bleached under blue light for 100 s at room
169 temperature, with an intervening gap of 1000 s, a set of four aliquots were later measured at
170 preheat temperatures from 160 to $260 \text{ }^\circ\text{C}$, with a step of $20 \text{ }^\circ\text{C}$. The results of the preheat
171 plateau tests (Fig. 2c) showed that the $D_{e,s}$ obtained by the SAR protocol are insensitive to
172 preheat temperature in range between $160 \text{ }^\circ\text{C}$ and $260 \text{ }^\circ\text{C}$. For both samples (MHN R2 and
173 ARR R4), all the recycling ratios are close to 1, while the recuperation values are less than
174 3%, especially at $160 \text{ }^\circ\text{C}$.

175 Young quartz samples may be affected by thermal transfer (Wintle and Murray, 2006). The
176 thermal transfer test as a function of preheat temperature was conducted for sample ARR R4
177 (Fig. 2d). The unheated aliquots were bleached twice under the blue light for 100 s at room
178 temperature with an intervening pause of 10 ks to allow charge optically transferred into the
179 $110 \text{ }^\circ\text{C}$ TL peak to decay. For sample ARR R4, four aliquots were determined at each preheat
180 temperature between $160 \text{ }^\circ\text{C}$ and $260 \text{ }^\circ\text{C}$ (in increments of $20 \text{ }^\circ\text{C}$). As shown in Fig. 2d, there
181 was no significant thermal transfer from $160 \text{ }^\circ\text{C}$ to $200 \text{ }^\circ\text{C}$. Based on the preheat plateau and
182 thermal transfer tests, a preheat temperature of $160 \text{ }^\circ\text{C}$ was selected for the quartz D_e
183 measurements.

184 The suitability of the procedure for D_e determination with the selected settings was checked
185 with a dose recovery test (Murray and Wintle, 2003). Nine natural aliquots of the sample
186 ARR R4 were stimulated twice by blue-light stimulation at $125 \text{ }^\circ\text{C}$ for 40 s. A laboratory dose
187 1.12 Gy was then administered, close to their expected natural $D_{e,s}$. The average dose
188 recovery ratio is 1.01 ± 0.01 , which shows the selected SAR protocol is suitable for D_e
189 determination.

190 4. Results

191 4.1 Quartz luminescence characteristics

192 The dose response curve and natural OSL decay curve (insert) of the representative samples
193 are shown in Fig. 2a and 2b. The decay curve of the samples resembles that of the calibration
194 quartz sample. The blue-light stimulated OSL signals decreased very quickly, which indicates
195 the OSL signals were fast-component dominated and that the sample was appropriate for OSL
196 dating (Jain et al., 2003). The regeneration dose of 0 Gy was used to measure recuperation,
197 which was calculated by comparing the sensitivity corrected OSL signal of the zero dose to
198 the sensitivity-corrected natural signal. Recuperation was in all cases <3% for all samples.
199 The recycling ratio, the consistency between the first regenerative dose and the repeated dose,
200 suggested that the sensitivity changes during analysis were adequately corrected. The
201 recuperation and recycling ratio show the reliability of the SAR protocol.

202 The preheat plateau tests indicated that the D_e s obtained by the SAR protocol are independent
203 of preheat temperature (Fig. 2c). The thermal transfer test shows the variations in D_e were
204 negligible from 160 °C to 200 °C, suggesting suitable preheating temperature range (Fig. 2d).

205 The D_e values are relatively low, and the majority of the D_e values fall in narrow range
206 between 0.04 and 1.40 Gy. The Abanico plot of D_e distributions (Dietze and Kreutzer, 2019)
207 of two representative samples (MHN R2 and ODE R10) display normal and narrow
208 distributions (Fig. 2e and 2f), indicating that the quartz particles were well bleached prior to
209 burial and the optical bleaching of the siliciclastic sediment in this study area was effective.
210 The study sediments may have experienced transportation mechanisms possibly from the
211 tidal current in the adjacent Atlantic Ocean, coupled with flood and erosion from the adjoined
212 basement complexes. Therefore, all the D_e for OSL ages calculation were acquired using the
213 average of twelve discs of each sample. The OSL dating results are summarized in Table 1.

214 4.2 OSL age of the sediments

215 The results of OSL age dating, including the dose rates, equivalent doses and ages are listed
216 in Table 1. The OSL ages are also displayed in the map (Fig. 3). The concentration of the
217 radioactive elements in the siliciclastic sediments are 0.36–10.1 ug/g (Th), 0.17–1.98 ug/g
218 (U) and 0.011–0.469% (K) with mean values of 2.275 ppm for Th, 0.49 ppm for U and 0.135
219 % for K, respectively. The water content ranged from 1 to 20 %. The time-averaged water
220 content available in the sediment throughout its burial is an important, but a difficult
221 parameter to assess (Cordier, 2010). Estimated value of the moisture content in these study

222 sediments may not be well indicative of the entire period of burial, but may reflect the
223 relative contribution to the effective dose rate. The dose rates range from $1.54 \pm 0.066 \text{ Gy ka}^{-1}$
224 to $0.22 \pm 0.041 \text{ Gy ka}^{-1}$, which are typical for coastal sediments (Kunz et al., 2010), and the D_e
225 values, from 1.4 ± 0.03 to $0.04 \pm 0.01 \text{ Gy}$. These yield OSL ages of the siliciclastic sediments
226 ranging from $3.52 \pm 0.34 \text{ ka}$ to $0.05 \pm 0.01 \text{ ka}$. The two oldest samples OKG R3 and MHN R2
227 have OSL ages of $3.52 \pm 0.34 \text{ ka}$ and $3.01 \pm 0.39 \text{ ka}$, respectively.

228 The OSL ages show that the deposits are of late Holocene. It was observed that the deposits
229 are thicker in northern part of the study area. The extent of sampling depth was constraint
230 with shallow groundwater table and showed no spatial trend (Fig. 3). However, the spatial
231 changes in age of the samples appear two belt-like distributions, with the exception of young
232 age ($1.55 \pm 0.15 \text{ ka}$ and 0.33 ± 0.08 , respectively) at the ORR and ZER barriers in the northeast
233 part of the study area. The inland belt has ages ranging from $3.01 \pm 0.39 \text{ ka}$ to $1.55 \pm 0.15 \text{ ka}$,
234 while the coast belt has ages ranging from $0.64 \pm 0.06 \text{ ka}$ to $0.05 \pm 0.01 \text{ ka}$. These two belts
235 approximately parallel to the coastline (Fig. 3). The ages of samples in this area yield a rate
236 of coastal progradation approximately 20 km in 3.5 ka, i.e. 5.7 km/ka.

237 5. Discussion

238 Ages of the study samples range from 3.52 ka to 0.05 ka. The result of OSL dating are
239 reliable as evidenced by the good dose recovery and a signal dominated by a fast component.
240 The very young age for the sediments is in contrast with some previous researches (Omatsola
241 and Adegoke, 1980; Billman, 1982), in which they used relative age dating techniques to
242 adopt a Tertiary age for the sediments. The Tertiary sediment could have experienced
243 reworked processes, transportation and re-deposited in the late Holocene. The variations in
244 ages of these samples might be an indication of various depositional episodes during the
245 Holocene epoch.

246 The thickness of the investigated siliciclastic sediments varies from 0.4 m to about 0.8
247 meters, while the deeper sediments could not be sampled in this study due to shallow
248 groundwater table in the region. The spatial changes in age of the samples appear two belt-
249 like distributions, with the exception of young age of the two samples in the hinterland (Fig.
250 3). Geomorphologically, the belts parallel to the barrier bars along coastlines. It is highly
251 possible that the sediments with age of 0.64 ka–0.05 ka in the belt close to the coastline have
252 disturbed by modern tide activities. Therefore, we mainly focus on the belt with age range of
253 3.52 ka–1.55 ka.

254 The deposition episode of 3.52 ka–1.55 ka could have resulted from one or combination of
255 two factors which include: 1) decrease in relative sea level; and 2) increase in flood activity.
256 Decrease in relative sea level is at least partly responsible for this deposition episode.
257 Decrease in relative sea level could be caused by basin uplift and/or decrease in sea level.
258 The knowledge of the tectonic movements in the region during the Holocene has been lacked.
259 Olabode (2015) analyzed tectonic evolution in the Dahomey Basin since Cretaceous, based
260 on data of one dimensional backstripping analysis on three offshore wells, and concluded that
261 the basin has been experienced accelerated tectonic subsidence during Quaternary period.
262 This may provide information of tectonic background for understanding the Holocene
263 sedimentation, but is contrary to the deposition episode in the interval 3.52 ka–1.55 ka that
264 suggests basin uplift.

265 Decrease in sea level may also contribute to the formation of sediment in this older hinterland
266 belt. However, it is generally accepted that global sea level has been increasing in the
267 Holocene, and there is a progressive decrease in rise rate from 6.7 ka to recent time, within
268 which main rise occurred in the interval 6.7–4.2 ka (Lambeck et al., 2014). Many physical
269 processes, such as crustal rebound, continental levering, ocean syphoning, etc., produce
270 distinctive spatial and temporal patterns in relative sea level during late Holocene (Barnett et
271 al., 2019). It is still an open question what specific mechanism that drive relative sea level in
272 the study region.

273 Increase in flood activity that brings materials for the sediment may be another factor,
274 although the supply of reworked Tertiary sediments can not be precluded. The rivers (Ofara,
275 Oluwa, Talita and Alape Rivers) drains across the study area. Salzmann and Hoelzmann,
276 based on pollen and geochemical analysis, showed in southern Benin of Gulf of Guinea, an
277 episode of wetting climatic conditions occurred between 3.3 ka and 1.1 ka. This is timely
278 consistent with age of sediments in the range of 3.52 ka–1.55 ka. It is possible that increased
279 river flooding during the wet period had brought more sediments deposited in the hinterland
280 of the study area, in addition to the reworked older sedimentary rocks.

281 Presently, it is difficult to determine which factors are responsible for the deposition episode
282 during the period of 3.52 ka–1.55 ka. Understanding of previous coastal fluctuations is
283 crucial to envisage the present dynamics of the coasts within the framework of long-term
284 fluctuations (Masselink and Gehrels, 2014). Depositional changes in the coasts occur relative
285 to many factors which includes: sea level fluctuation, basin uplift, flood and sediment supply,
286 climate and human activity. Past changes associated with variations in these factors may

287 inform our understanding of future changes in the coast area. Further investigations with
288 large spatiotemporal coverage in the region are needed in future to better understand the past
289 dynamics of the coasts in the region.

290 **6. Conclusion**

291 This study presents the first OSL dating of the coastal sediments, with large spatial coverage
292 in the eastern Dahomey Basin. The OSL results revealed that the ages of the surficial
293 sediments in the eastern basin range from 3.5 ka to 0.05 ka, indicating that the deposits are
294 very young Quaternary deposits, specifically of Holocene Epoch. The young ages contradict
295 the assertion of some previous researcher (Billman, 1982) who adopt a Tertiary age for the
296 sediments using relative age dating techniques. The age of the sediments varies spatially from
297 the northeast to southwest of the study area, indicating the sediments are result of the
298 regressive depositional episodes that occurred in the study area. The decrease in relative sea
299 level and/or in river flooding during the wet climatic conditions may be responsible for the
300 elder deposition episode of 3.5-1.5 ka in the region. Therefore, this study provides first
301 chronological constraints on evolution of the coast area and the linkage with relative sea level
302 changes (linked with both the sea level and tectonics) during the late Holocene.

303 **Author contributions**

304 Richard O. Fakolade: Investigation, Writing - Original Draft, Visualization. Philip R. Ikhane:
305 Conceptualization, Writing - Review & Editing, Supervision. Qiuyue Zhao:
306 Conceptualization, Methodology, Writing - Review & Editing, Supervision. Qingzhen Hao:
307 Conceptualization, Validation, Resources, Writing - Review & Editing, Supervision, Project
308 administration, Funding acquisition. Helena Alexanderson: Methodology, Editing. Zhengtang
309 Guo: Conceptualization, Validation, Resources, Writing – Review & Editing, Funding
310 acquisition.

311 **Data availability**

312 All data included in this study are available upon request by contact with the corresponding
313 author.

314 **Acknowledgements**

315 We are grateful to two anonymous reviewers for their constructive comments and suggestions
 316 that significantly improve the manuscript. This study was supported by the National Natural
 317 Science Foundation of China (Grants 41888101 and 41625010). O. R., Fakolade would like
 318 to thank all graduate students of Professor Q. Hao of the Key Laboratory of Cenozoic
 319 Geology and Environment, Institute of Geology and Geophysics, Chinese Academy of
 320 Sciences for the research collaborative program with Olabisi Onabanjo University Ago
 321 Iwoye. Appreciation goes to all lecturers and staff of the Department Earth Sciences Olabisi
 322 Onabanjo University Ago Iwoye for the contribution to the success of the project.

323 **References**

- 324 Adamiec, G., Aitken M.J., 1998. Dose rate conversions factors: update. *Ancient TL*, 16, 37–
 325 50.
- 326 Adegoke, O. S., 1969. Eocene stratigraphy of Southern Nigeria. *Mem. Bur. Rech. Geol.*
 327 *Mins.*, 23–46.
- 328 Adegoke, O.S., 1980. Relevant geosciences. *Discussion*, Nigeria Academy of Science, 31–33.
- 329 Adekeye, O. A., 2004. Aspect of sedimentology, geochemistry and hydrocarbon potentials of
 330 Cretaceous-Tertiary sediments in Dahomey Basin, South-western Nigeria. Unpublished
 331 Ph.D. thesis, University of Ilorin, 202p.
- 332 Adekeye, O.A., Akande, S.O., Erdtman, B.D., Samuel, O.J., Hetenyi, M., 2006. Hydrocarbon
 333 potential Assessment of the Upper Cretaceous-Lower Tertiary sequence in the Dahomey
 334 Basin Southwestern Nigeria. *NAPE Bulletin*, 19 (1), 50–60.
- 335 Agagu, O.A., 1985. A geological guide to Bituminous sediments in Southwestern Nigeria.
 336 Unpublished Report, Department of Geology University of Ibadan.
- 337 Aitken, M.J., 1985. *Thermoluminescence dating*. Academic Press, London, 359 p.
- 338 Aitken, M.J., 1998. *An introduction to optical dating*. Oxford University press, Oxford, 267 p.
- 339 Awosika, L., Folorunsho, R., 2010. The Ocean Data and Information Network of Africa.
 340 Nigerian Institute for Oceanography and Marine Research, 1, 128–132.
- 341 Bailey, R.M., Smith, B.W., Rhodes, E.J., 1997. Partial bleaching and the decay form
 342 characteristics of quartz OSL. *Radiation Measurements*, 27, 123–136.
- 343 Barnett, R.L., Bernatchez, P., Garneau, M., Brain, M. J., Charman, D. J., Stephenson, D.B.,
 344 Haley, S., Sanderson. N., 2019. Late Holocene sea-level changes in eastern QuEbec and
 345 potential drivers. *Quaternary Science Reviews*, 203, 151–169.

- 346 Billman, H.G., 1982. Offshore Stratigraphy and Paleontology of Dahomey Embayment, West
347 Africa. Nigerian Association of Petroleum Explorationists Bulletin, 7, 121–130.
- 348 Bøtter-Jensen, L., Duller, G.A.T., Poolton, N.R.J., 1994. Excitation and emission
349 spectrometry of stimulated luminescence from quartz and feldspars. Radiation
350 Measurements, 23, 613–616.
- 351 Buylaert, J.P., Murray, A.S., Vandenberghe, D., Vriend, M., De Corte, F., Van den haute, P.,
352 2008. Optical dating of Chinese loess using sand-sized quartz: establishing a time frame
353 for Late Pleistocene climate changes in the western part of the Chinese Loess Plateau.
354 Quat. Geochronology, 3, 99–113.
- 355 Chen, Y., Li, S.-H., Li, B., Hao, Q., Sun, J., 2015. Maximum age limitation in luminescence
356 dating of Chinese loess using the multiple-aliquot MET-pIRIR signals from K-feldspar.
357 Quaternary Geochronology, 30, Part B, 207–212.
- 358 Cordier, S., 2010. Optically stimulated luminescence dating: procedures and applications to
359 geomorphological research in France. Géomorphologie: Relief, Processus,
360 Environnement, (1), 21–40.
- 361 Dietze, M., Kreutzer, S., 2019. Plot_AbanicoPlot: function to create an Abanico plot.
362 Function version 0.1.10. In: Kreutzer, S., Burow, C., Dietze, M., Fuchs, M.C., Schmidt,
363 C., Fischer, M., Friedrich, J. (Eds.) Luminescence: Comprehensive Luminescence
364 Dating Data Analysis. R package version 0.9.0.109.
- 365 Duller, G.A.T., 2003. Distinguishing quartz and feldspars in single grain luminescence
366 measurements. Radiation Measurements, 37, 161–165.
- 367 Elueze, A.A., Nton, M.E., 2004. Composition characteristics and industrial assessment of
368 sedimentary clay bodies in part of eastern Dahomey Basin, Southwestern Nigeria. J. Min.
369 and Geol., 4 (12), 175–184.
- 370 Guerin, G., Mercier, N., Nathan, R., Adamiec, G., Lefrais, Y., 2012. On the use of the infinite
371 matrix assumption and associated concepts: a critical review. Radiat. Meas., 47 (9), 778–
372 785.
- 373 Idowu, J.O., Ajiboye, S. A., Ilesanmi, M. A., Tanimola A., 1993. Origin and significance of
374 organic matter of Oshosun Formation Dahomey Basin Nigeria. Journal of Min. Geol.,
375 29, 9–27.
- 376 Ikhane, P. R., Akintola, A. I., Bankole, S. I., Oyinboade, Y. T., 2014. Provenance studies of
377 sandstone facies exposed near Igbile Southwestern Nigeria: petrographic and
378 geochemical approach. Journal on Geography and Geology, 6 (2), 47–60.

- 379 Jain, M., Murray, A.S., Bøtter-Jensen, L., 2003. Characterisation of blue-light stimulated
380 luminescence components in different quartz samples: implications for dose
381 measurement. *Radiation Measurements*, 37, 441–449.
- 382 Jain, M., Murray, A. S., Bøtter-Jensen, L., 2004. Optically stimulated luminescence dating:
383 how significant is incomplete light exposure in fluvial environments? *Quaternaire*, 15,
384 143–157.
- 385 Jones, H.A., Hockey, R.D., 1964. The geology of part of southwestern Nigeria. *Geological*
386 *Survey of Nigeria Bulletin*, 31, 335–336.
- 387 Kang, S.G., Wang, X.L., Lu, Y.C., 2013. Quartz OSL chronology and dust accumulation rate
388 changes since the Last Glacial at Weinan in the southeastern Chinese Loess Plateau.
389 *Boreas*, 42, 815–829.
- 390 Kingston, D. R., Dishroon, C. P., Williams, P. A., 1983. Global Basin Classification System.
391 *AAPG. Bull.* 67, 2175–2193.
- 392 Kunz, A, Frechen, M, Ramesh, R., Urban, B. 2010. Periods of recent dune sand mobilisation
393 in Cuddalore, Southeast India. *Zeitschrift der Deutschen Gesellschaft für*
394 *Geowissenschaften*, 161, 353–368.
- 395 Lai, Z.P. and Wintle, A.G., 2006. Locating the boundary between the Pleistocene and the
396 Holocene in Chinese loess using luminescence. *The Holocene*, 16, 893–899.
- 397 Lai, Z.P., 2010. Chronology and the upper dating limit for loess samples from luochuan
398 section in the Chinese loess plateau using quartz OSL SAR protocol. *I. Asian Earth Sci.*,
399 37, 176–185.
- 400 Lambeck, K., Rouby, H., Purcell, A., Sun, Y., Sambridge, M., 2014. Sea level and global ice
401 volumes from the last glacial maximum to the Holocene. *Proc. Natl. Acad. Sci. Unit.*
402 *States Am.* 111 (43), 15296–15303.
- 403 Masselink, G., Gehrels, R., 2014. *Coastal Environments and Global Change*. John Wiley &
404 Sons, West Sussex, UK, 448 p.
- 405 Mpanda, S., 1997. Geological development of East Africa coastal basin of Tanzania. *Acta*
406 *Universities Stockhomiensis*, 45, 121p.
- 407 Murray, A.S., Wintle, A.G., 2000. Luminescence dating of quartz using an improved single
408 aliquot regenerative-dose protocol. *Radiation Measurements*, 32, 57–73.
- 409 Murray, A.S., Wintle, A.G., 2003. The single aliquot regenerative dose protocol: potential for
410 improvements in reliability. *Radiation Measurements*, 37, 377–381.

- 411 Nton, N.E., Ikhane, P.R., Tijani, M.N., 2006. Aspect of rock-eval studies of the Maastrichtian-
412 Eocene sediments from subsurface, in the eastern Dahomey Basin, Southwestern
413 Nigeria. *European Journal of Scientific Research*, 25 (3), 417–427.
- 414 Okosun, E.A. 1990. A review of the cretaceous stratigraphy of the Dahomey Embayment,
415 West Africa. *Cretaceous Research*, 11, 17–27.
- 416 Olabode, S.O., 2015. Subsidence Patterns in the Nigerian sector of Benin (Dahomey) Basin:
417 Evidence from three offshore wells. *Ife Journal of Science*, 17 (2), 23–35.
- 418 Olabode, S.O., Mohammed, M.Z., 2016. Depositional facies and sequence stratigraphic study
419 in parts of Benin (Dahomey) Basin SW Nigeria: Implications on the Reinterpretation of
420 Tertiary Sedimentary Successions. *International Journal of Geosciences*, 7, 210–228.
- 421 Olley, J.M., Caitcheon, G.G., Murray, A.S., 1998. The distribution of apparent dose as
422 determined by optically stimulated luminescence in small aliquots of fluvial quartz:
423 implications for dating young sediments. *Quaternary Science Reviews*, 17, 1033–1040.
- 424 Olley, J.M., Caitcheon, G., Roberts R.G., 1999. The origin of dose distributions in fluvial
425 sediments, and the prospect of dating single grains of quartz from fluvial deposits using
426 OSL. *Radiation Measurements*, 30, 207–217.
- 427 Omatsola, M.E., Adegoke O.S., 1981. Tectonic evolution and cretaceous stratigraphy of the
428 Dahomey basin Nigeria. *Journal Mining and Geology*, 18 (1), 130–137.
- 429 Prescott, J.R., Hutton, J.T., 1994. Cosmic ray contribution to dose rates for luminescence and
430 ESR dating: large depths and log-term time variations. *Radiation Measurements*, 23,
431 497–500.
- 432 Reyment, R.A., 1965. Aspects of the geology of Nigeria: The stratigraphy of the Cretaceous
433 and Cenozoic deposits. Ibadan University Press, 133p.
- 434 Rittenour, T.M., 2008. Luminescence dating of fluvial deposits: applications to geomorphic,
435 paleo-seismic and archaeological research. *Boreas*. 37, 613–635.
- 436 Roberts, H. M., 2007. Assessing the effectiveness of the double-SAR protocol in isolating a
437 luminescence signal dominated by quartz. *Radiation measurements*, 42, 1627–1636.
- 438 Roberts, H.M., Duller, G.A.T., 2004. Standardised growth curves for optical dating of
439 sediment using multiple-grain aliquots. *Radiat. Meas.* 38, 241–252.
- 440 Rodnight, H., Duller, G.A.T., Wintle, A.G., Tooth, S., 2006. Assessing the reproducibility and
441 accuracy of optical dating of fluvial deposits. *Quaternary Geochronology*, 1, 109–120.

- 442 Salzmann, U., Hoelzmann, P., 2005. The Dahomey Gap: an abrupt climatically induced rain
443 forest fragmentation in West Africa during the late Holocene. *The Holocene*, 15 (2), 190
444 –199.
- 445 Stokes, S. 1999. Luminescence dating applications in geomorphological research.
446 *Geomorphology*, 29, 153–171.
- 447 Stokes, S., Bray H.E., Blum, M.D., 2001. Optical resetting in large drainage basin: tests of
448 zeroing assumptions using single aliquots procedures. *Quaternary Science Reviews*, 20,
449 879–885.
- 450 Udo-Akuaibit, S.P., 2017. Sea-level rise and coastal submergence along the south east coast
451 of Nigeria. *J. Oceanogr. Mar. Res.*, 5, 172. doi: 10.4172/2572-3103.1000172.
- 452 Wang, X.L., Lu, Y.C., Wintle, A.G., 2006. Recuperated OSL dating of fine grained quartz in
453 Chinese loess. *Quaternary Geochronology*, 1, 89–100.
- 454 Whiteman, A.J., 1982. Nigeria: its Petroleum Geology, Resources and Potential. Graham and
455 Trotman limited, London, 1 (2), 166p.
- 456 Wintle, A.G., 1997. Luminescence dating: laboratory procedures and protocols. *Radiation*
457 *Measurements*, 27, 769–817.
- 458 Wintle, A.G., 2008. Fifty years of luminescence dating. *Archaeometry*, 50, 276–312.
- 459 Wintle, A.G., Murray A.S., 2006. A review of quartz optically stimulated luminescence
460 characteristics and their relevance in single aliquot regeneration dating protocols.
461 *Radiation Measurements*, 41, 369–391.
- 462 Woodroffe, S. A., Horton, B. P., 2005. Holocene sea-level changes in the Indo-Pacific.
463 *Journal of Asian Earth Sciences*, 25 (1), 29–43.
- 464 Yang, S.L., Forman, S.L., Song, Y.G., Pierson, J., Mazzocco, J., Li, X.X., Shi, Z.T., Fang,
465 X.M., 2014. Evaluating OSL-SAR protocols for dating quartz grains from the loess in Ili
466 Basin, Central Asia. *Quaternary Geochronology*, 20, 78–88.
- 467 Zhang, J., Li, S.H., Sun, J., Hao, Q., 2018. Fake age hiatus in a loess section revealed by OSL
468 dating of calcrete nodules. *Journal of Asian Earth Sciences*, 155, 139–145.
- 469 Zhao, Q.Y., Thomsen, K. J., Murray, A. S., Wei, M.J., Pan, B.L., Song, B., Zhou, R., Chen,
470 S.Z., Zhao, X.H., Chen, H.Y., 2015. Testing the use of OSL from quartz grains for dating
471 debris flows in Miyun, northeast Beijing, China. *Quaternary Geochronology*, 30, 320–
472 327.
- 473 Zhao, Q., Thomsen, K. J., Murray, A. S., Wei, M., Song, B., 2017. Single-grain quartz OSL
474 dating of debris flow deposits from Men Tou Gou, south west Beijing, China.
475 *Quaternary Geochronology*, 41, 62–69.

476

477 **Figure Captions**

478 **Figure 1.** Maps of the study area (Modified after NGSAs, 1969).with locations of the OSL
479 samples.

480 **Figure 2.** Quartz luminescence characteristics of the representative samples. (a) and (b) Dose
481 response curves of the typical samples OKG R3 and AGG R8, respectively. Inset shows
482 the natural decay curves. (c) D_e values versus preheat plateau tests for two typical
483 samples of MHA R2 and ARR R4. (d) Thermal transfer test of the typical sample ARR
484 R4. (e) and (f) The Abanico plot of D_e distributions of two typical samples MHN R2 and
485 ODE R10, respectively.

486 **Figure 3.** Map of study area showing the OSL ages. The zone outlined by yellow line
487 indicate the first episode of sedimentation in mostly of barrier bar, and the zone outlined
488 by blue line indicate littoral zone.

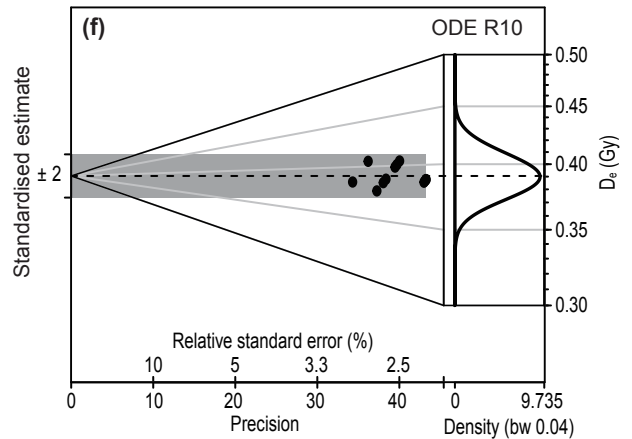
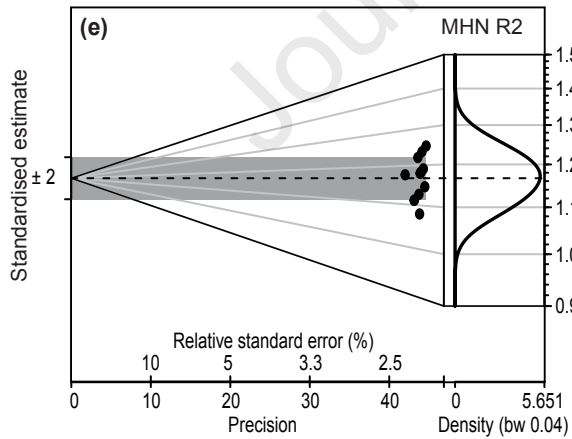
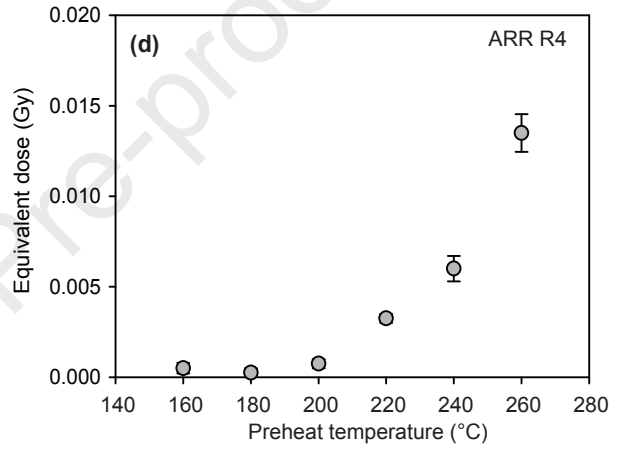
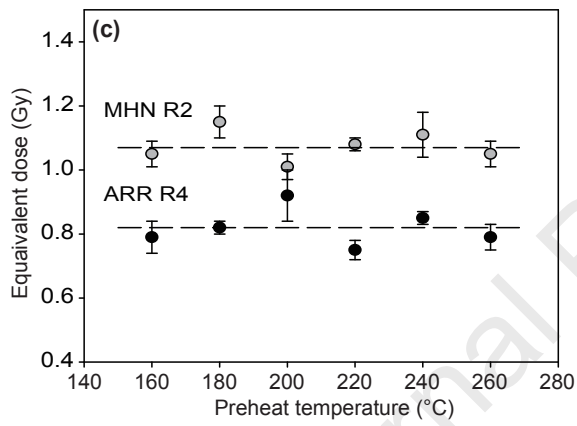
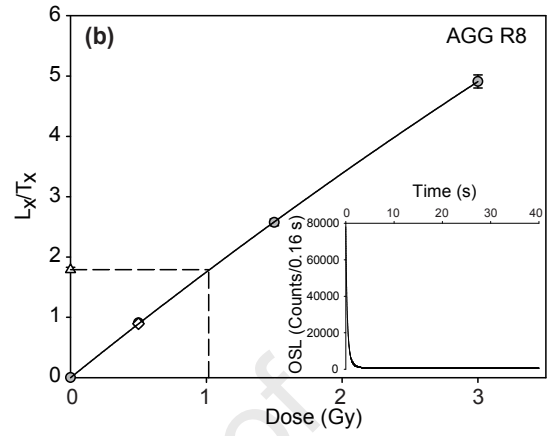
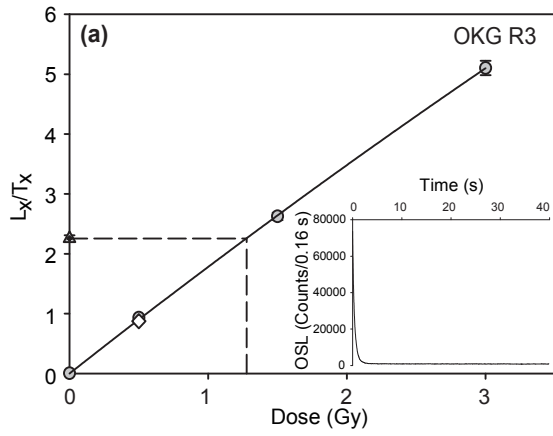
489

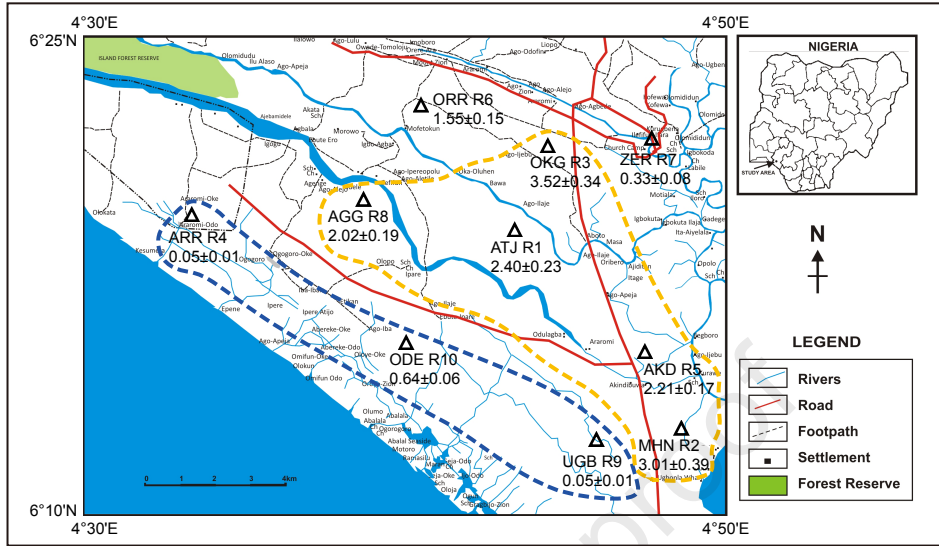
490 **List of Table**

491 **Table 1.** Summary of sample location, the burial depth, radionuclide concentrations,
492 calculated dose rate, quartz D_e values and luminescence ages.

Sample code	Latitude (°N)	Longitude (°E)	Altitude (m)	Depth (m)	Grain size (µm)	Water content (%)	U (µg/g)	Th (µg/g)	K (%)	D _e (Gy)	Dose rate (Gy/ka)	Age (ka)
ATJ R1	6.31	4.75	6.00	0.80	150–200	4.0	0.32	1.61	0.054	0.93±0.03	0.39±0.035	2.40±0.23
MHN R2	6.20	4.78	3.20	0.50	150–200	3.0	0.17	1.25	0.011	1.17±0.02	0.39±0.049	3.01±0.39
OKG R3	6.38	4.76	7.60	0.60	200–250	14.0	0.35	1.55	0.011	1.40±0.03	0.40±0.037	3.52±0.34
ARR R4	6.34	4.49	1.46	0.45	200–250	6.0	1.98	10.70	0.216	0.08±0.01	1.54±0.066	0.05±0.01
AKD R5	6.26	4.77	1.97	0.60	150–200	14.0	0.58	1.19	0.090	1.08±0.02	0.49±0.036	2.21±0.17
ORR R6	6.38	4.74	8.50	0.60	150–200	1.0	0.29	2.01	0.024	0.76±0.03	0.49±0.043	1.55±0.15
ZER R7	6.38	4.78	9.40	0.80	150–200	18.0	0.21	0.49	0.011	0.07±0.01	0.22±0.041	0.33±0.08
AGG R8	6.31	4.63	10.40	0.40	150–200	8.0	0.34	0.36	0.175	1.00±0.03	0.50±0.044	2.02±0.19
UGB R9	6.15	4.79	27.20	0.45	200–250	12.0	0.24	1.91	0.469	0.04±0.01	0.79±0.039	0.05±0.01
ODE R10	6.29	4.62	8.50	0.50	150–200	20.0	0.42	1.50	0.299	0.39±0.03	0.61±0.034	0.64±0.06







Declaration of interests

The authors declare that they have no known competing financial interests or personal relationships that could have appeared to influence the work reported in this paper.

The authors declare the following financial interests/personal relationships which may be considered as potential competing interests:

Qingzhen Hao

Journal Pre-proof